Defects in the Compound Bi₂Te₃ Caused by Irradiation with Protons

P. Chaudhari* and Michael B. Bever

Department of Metallurgy and Center for Materials Science and Engineering
Massachusetts Institute of Technology
Cambridge, Massachusetts

Abstract

Single crystal foils of the compound Bi_2Te_3 were irradiated with 7.5 MeV protons at two levels of flux to the same integrated dose of 5.5×10^{18} protons/cm^2. The specimens were examined by transmission electron microscopy. After irradiation with a flux of 1.8×10^{13} protons/cm^2-sec, clusters of point defects ranging in size from approximately 50 to 250 A.U. were observed. These clusters annealed out during examination in the electron microscope. After irradiation with a flux of 3.0×10^{13} protons/cm^2-sec, clusters of interstitial atoms and clusters of vacancies could be distinguished. Hexagonal areas were observed after irradiation with the higher flux. Irradiation also promoted the rearrangement of dislocations. Segments of dislocations intersected the surface of the specimens and dislocations acquired a jagged appearance.

* Present address: Thomas J. Watson Research Center, IBM, Yorktown Heights, New York.

I. INTRODUCTION

The effects of irradiation with gamma rays, electrons, neutrons and protons on the electrical properties of the compound Bi_2Te_3 have been investigated.[1-7] These investigations show that the transport properties of Bi_2Te_3 are sensitive to the defects generated during irradiation. It has also been found that some of the defects are mobile at or slightly above room temperature. For example, heating to $50^\circ C$ changed the Hall coefficient and electrical resistivity of specimens of Bi_2Te_3, which had been exposed to gamma radiation; these changes were attributed to the dissociation of interstitial clusters and the migration of interstitials.[2]

The work reported here is part of an investigation of the effects of irradiation with protons of 7.5 MeV energy on the compound Bi_2Te_3. In an earlier paper, the value of the number of defects obtained from the changes in the electrical properties was more than an order of magnitude smaller than values calculated from theories of radiation damage.[7] The annealing out of defects during irradiation was considered to be one of the reasons for this difference. If the defects can migrate and a sufficient supersaturation of point defects is generated by the irradiation, defect clusters should be formed. Transmission electron microscopy is suitable for the direct observation of ·such clusters. It also can provide information about the structural relations of the clusters and the matrix and, under certain conditions, about the types of point defects forming the cluster.

The structure of the compound Bi_2Te_3 is rhombohedral;[8] it will be analyzed here in terms of the hexagonal system. The length of the

a-axis is 4.3835 A.U. and that of the c-axis 30.487 A.U.[9] The

compound has a layer structure, in which the layers are stacked along

the c-axis. Units of five layers are repeated; the stacking sequence

of such a unit is:

$$-Te(1) - Bi - Te(2) - Bi - Te(1) -$$
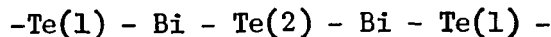
The bonding scheme of Bi_2Te_3 consists of van der Waals bonding

between atoms in neighboring Te(1) layers, mixed covalent and ionic

bonding between atoms in neighboring Te(1) and Bi layers, and covalent

bonding between atoms in neighboring Te(2) and Bi layers.[10] Because

of the weak bonding between Te(1) layers, the compound cleaves easily.

The compound Bi_2Te_3 has been investigated by transmission electron

microscopy. Dislocations with a Burgers vector $<2\bar{1}\bar{1}0>$ have been observed.[11]

In the solid solution alloys of Bi_2Te_3 and Sb_2Te_3 in the range between

pure Sb_2Te_3 and 40 pct Sb_2Te_3-60 pct Bi_2Te_3, dislocation loops have been

observed on basal planes; these loops have been attributed to deviations

from stoichiometry.[12,13] Although deviations from the stoichiometric

composition occur in pure Bi_2Te_3 and are responsible for its p-type

behavior,[14] coalescence of these point defects has not been observed.

II. EXPERIMENTAL PROCEDURE

Foils of the compound Bi_2Te_3 suitable for transmission electron

microscopy were prepared by cleaving a single crystal with Scotch tape.[11]

The foils were placed between folded gold grids. Specimens were

examined in a Siemens Elmiskop I microscope or a Hitachi HU-11 micro-

scope before irradiation.

The specimens held between the folded gold grids were placed on the water-cooled target support shown in Fig. 1. An aluminum foil, 5×10^{-4} cm thick, covering the grids kept them firmly in place. After the assembled target was placed in the internal beam chamber of the cyclotron, the chamber was evacuated. It should be emphasized that the specimens were not cooled uniformly during irradiation because the areas in direct contact with the metal in the grids were cooled more efficiently than areas facing the openings.

From the changes in the Hall coefficient and electrical resistivity of the specimens irradiated in a similar manner, it was calculated that a proton in a centimeter of travel generates approximately 580 defects.[7] In order to obtain a sufficiently high concentration of point defects, the integrated dose used in the irradiation of specimens for examination by electron microscopy was 5.5×10^{18} protons/cm^2 and the level of the flux was more than an order of magnitude higher than that used in irradiating specimens for the electrical measurements.[7] As explained in the earlier paper, the flux and the integrated dose may be consistently in error by 20-30 pct.

Two batches of several specimens each were irradiated at two levels of flux to the same integrated dose. During irradiation the specimens were oriented so that their c-axis was parallel to the proton beam. After irradiation, the specimens were held at $78^{\circ}K$ for at least seven days to allow the induced radioactivity to decay. The specimens were then examined by electron microscopy.

The diffraction pattern of the selected area and the bright-field image corresponding to this area were rotated with respect to each other

through the required angle to eliminate the rotation of the image relative to the diffraction pattern.[15] The rotation includes an 180° inversion which arises through differences in intermediate lens excitation between the diffraction and imaging operations.[16]

III. RESULTS AND DISCUSSION

The types of defect clusters observed after the irradiation were different for the two levels of flux. This was due to the difference in the concentrations of point defects generated per unit time and to the difference in the temperature of the specimen during irradiation.

The preparation of foils for transmission electron microscopy by the cleavage technique introduced a large number of dislocations. The arrangement of these dislocations into networks was similar to that already reported in the literature.[11] Since in the presence of excess vacancies and interstitials generated by the irradiation, edge dislocations can move nonconservatively, some rearrangement was expected and was in fact observed.

A. Point Defects

Irradiation with a Flux of 1.8 x 10^{13} Protons/cm²-sec — Defect clusters ranging in size from 50 to 250 A.U. were visible in the electron microscope. Such clusters appear as dark spots in Fig. 2(a)-(d). The foils were so oriented in the electron microscope that the c-axis of the specimen was parallel to the electron beam. In this orientation, some of the clusters had their longest dimension parallel to the <10$\bar{1}$0> and <11$\bar{2}$0> directions. In Fig. 2(a) some spots which are aligned in the <11$\bar{2}$0> direction are marked A and some spots aligned in the <10$\bar{1}$0>

direction are marked B. The defect clusters were observed to anneal out in the microscope, presumably because of the temperature rise caused by the electron beam. The sequence of electron micrographs in Fig. 2(a)-(d) illustrates the progressive annealing out of the clusters.

The shape of the defect clusters is determined by the type of the bonds present in the compound. Because of the directional nature of the predominating covalent bond in the compound Bi_2Te_3, the smaller clusters may be expected to have shapes other than spherical. The alignment of the major axis of these clusters in the $\langle 10\bar{1}0 \rangle$ and $\langle 11\bar{2}0 \rangle$ directions is probably connected with this factor. If the size of a cluster increases, it may lower its energy by collapsing into a dislocation loop. In the compound Bi_2Te_3 vacancy clusters can collapse into dislocation loops lying on three of the six $\{20\bar{2}9\}$ planes. In loops lying on these planes the largest number of bismuth-tellurium bonds broken are in the plane of the loop and the disruption of the structure is least severe. If a Shockley partial dislocation is nucleated on the periphery of such a loop, the broken bonds on one side of the loop can combine with those on the other side. The projection of such a circular loop on the basal plane would be an ellipse with a major axis along the $\langle 11\bar{2}0 \rangle$ direction.

Several dislocation loops can be seen in Fig. 3. From measurements of the lengths of the major and minor axes of the ellipse, the angle of inclination of the plane of the loop to the basal plane can be estimated. This angle was approximately equal to the angle between the $\{20\bar{2}9\}$ and the basal planes. Loops of the type shown in Fig. 3 appeared less frequently than the dark spots.

<u>Irradiation with a Flux of 3.0 x 10^{13} Protons/cm^2-sec.</u> - The
defect clusters observed as dark spots after irradiation with a flux
of 1.8 x 10^{13} protons/cm^2-sec were not seen after irradiation with
the higher flux. They probably had annealed out during irradiation
because of the increase in temperature caused by the higher flux.

The defect clusters present after irradiation at the higher flux
are shown in Fig. 4. The defect clusters marked I in Fig. 4(a) show
a line of no contrast perpendicular to the diffraction vector. The
line of no contrast satisfies the condition $\vec{g} \cdot \vec{b} = 0$, where $\vec{g}$ is the
diffraction vector and $\vec{b}$ is the Burgers vector.[17] Rotating the
diffraction vector causes a corresponding rotation of the line of
no contrast. The line of symmetry cutting across the pairs of crescents
in Fig. 4(a) and (b) is parallel to the diffraction vector and indicates
that the strain field of the defect is symmetrical about the c-axis of
the specimen.[18]

As the specimens were much thicker than the extinction distance,
dynamical diffraction gave rise to the observed contrast effects.
Defect clusters lying close to a surface can be identified by dark
field microscopy.[18] Fig. 4(c) shows a dark field image of the same
area as that in Fig. 4(b); the spots marked I and V are identified as
clusters of interstitials and clusters of vacancies.

The interstitial clusters marked I in Fig. 4 are not dislocation
loops, but may be considered as coherent precipitates. A dislocation
loop lying on the basal plane with a Burgers vector parallel to the
c-axis does not produce diffraction contrast when the electron beam
is parallel to the c-axis. The interstitial clusters shown in Fig. 4

must therefore have components of the Burgers vector in the plane of the foil. Since the contrast effects of the interstitial clusters are symmetrical about the c-axis, the clusters are not prismatic dislocation loops. The interstitial atoms present in the clusters must therefore modify the bonding scheme locally so as to form precipitates, which are coherent with the lattice.

Pairs of loops of the type shown in Fig. 3 and agglomerations of defect clusters as that marked X in Fig. 4 were occasionally observed. Both types of observations probably arise from the interaction of stresses around the defect clusters causing them to migrate towards each other.[19]

In some areas of specimens associated light and dark regions and small light regions having hexagonal symmetry were seen and are illustrated in Fig. 5. If the beam current of the electron microscope was slowly increased so as to raise the temperature of the specimen, the hexagonal areas (marked B in Fig. 5) were observed to grow. The micrographs in Fig. 5(a)-(c) record such a sequence. Small light spots (marked C) were also observed to grow into larger areas with hexagonal symmetry. Some of the hexagonal areas assumed triangular shapes. An example of this is the area marked A in Fig. 5(a), (b) and (c). The sides of the hexagonal and the triangular areas were parallel to one of the $\langle 11\bar{2}0 \rangle$ directions.

The associated light and dark regions and the light regions may have been due to a combination of the high temperature and the defects introduced by the protons near the surface, which led to local evaporation of material because of the high vacuum. The growth of these

regions observed in the electron microscope may have been due to further evaporation from the edge created by the initial evaporation. That irradiation was necessary for these effects was confirmed by heating unirradiated specimens in high vacuum.

B. Dislocations

The arrangement of dislocations in Bi_2Te_3 is affected by the point defects generated and the temperature rise of the specimen during irradiation. Examples of these effects can be seen in Figs. 2, 3, 4 and 6.

In irradiated specimens short segments of some dislocation lines showed no diffraction contrast. An example is the segment of the dislocation line marked S in Fig. 6. This micrograph also illustrates the effect of irradiation on a dislocation network. Some of the dislocations forming the network intersect the surface of the specimen at such points as P. During examination in the microscope, dislocations, one end of which intersected the surface, reduced their length. An example is the dislocation marked D in the sequence of micrographs in Fig. 2(a)-(d). Similar observations of dislocation movement in the electron microscope have been reported for unirradiated specimens of Bi_2Te_3.[11]

In the unirradiated specimens the dislocation lines were smooth and generally tended to be parallel to each other. After irradiation these lines became jagged although they remained approximately parallel. This can be seen in Figs. 4 and 6. Nonuniform cooling of the specimens during irradiation set up stresses which presumably caused the dislocations to move. On completion of the irradiation and removal of

the stresses due to thermal gradients the dislocations tended to move
back toward their original positions. However, the defect clusters
generated by the irradiation and the presence of jogs on the dislocation
lines pinned the dislocations and gave rise to their jagged appearance.

IV. SUMMARY AND CONCLUSIONS

The defect clusters formed by irradiating specimens of the compound
Bi_2Te_3 with 7.5 MeV protons have been examined by transmission electron
microscopy. The effect of irradiation on the dislocations has also
been investigated.

After irradiation with a flux of 1.8×10^{13} protons/cm^2-sec to an
integrated dose of 5.5×10^{18} protons/cm^2, clusters of point defects
ranging in size from 50 to 250 A.U. were observed. These clusters an-
nealed out during examination in the electron microscope. Some of the
clusters were aligned along the $<10\bar{1}0>$ or the $<11\bar{2}0>$ directions.

After irradiation with a flux of 3.0×10^{13} protons/cm^2-sec to an
integrated dose of 5.5×10^{18} protons/cm^2, clusters of interstitial
atoms and clusters of vacancies could be distinguished. The interstitial
clusters probably were coherent precipitates.

Areas with hexagonal shapes in which the sides were parallel to the
$<11\bar{2}0>$ direction were observed in some parts of the specimens irradiated
with a flux of 3.0×10^{13} protons/cm^2. During examination in the electron
microscope at high electron beam currents, these areas were observed
to grow and some changed from hexagonal to triangular shapes. The areas
are tentatively explained by local evaporation of material at defects at
the surface at the temperature and vacuum during irradiation in the cyclotron.

Irradiation promoted dislocation rearrangement. Segments of dis-
locations intersected the surface of the specimens and dislocations
acquired a jagged appearance because of pinning by defect clusters
generated during irradiation.

ACKNOWLEDGMENTS

REFERENCES

1. R. A. Artman and A. N. Goland: Bull. Am. Phys. Soc. $\underline{5}$, 168 (1960).

2. M. J. Smith: J. Appl. Phys. $\underline{34}$, 2879 (1963).

3. R. A. Levy: Bull. Am. Phys. Soc. $\underline{5}$, 168 (1960).

4. J. C. Corelli, R. T. Frost and F. A. White: Bull. Am. Phys. Soc. $\underline{5}$, 168 (1960).

5. M. Balicki, J. C. Corelli and R. T. Frost: "Metallurgy of Elemental and Compound Semiconductors," (Interscience Publishers, Inc., New York) Vol. 12, (1961).

6. R. A. Artman and A. N. Goland: Bull. Am. Phys. Soc. $\underline{7}$, 187 (1962).

7. P. Chaudhari and M. B. Bever: J. Appl. Phys. $\underline{37}$, 4181 (1966).

8. R. P. W. Lange: Naturwiss. $\underline{27}$, 133 (1939).

9. M. H. Francombe: British J. Appl. Phys. $\underline{9}$, 415 (1958).

10. J. R. Drabble and G. H. Goodman: J. Phys. Chem. Solids $\underline{5}$, 142 (1958).

11. P. Delavignette and S. Amelinckx: Phil. Mag. $\underline{5}$, 729 (1960).

12. P. Delavignette and S. Amelinckx: Phil. Mag. $\underline{6}$, 601 (1961).

13. J. N. Bierly: Proc. 5th Intern. Conf. on Electron Microscopy, Philadelphia, $\underline{1}$, J-14 (1962).

14. G. R. Miller and Che-Yu. Li: J. Phys. Chem. Solids $\underline{26}$, 173 (1965).

15. P. B. Hirsch, A. Howie, R. B. Nicholson, D. W. Pashley and M. J. Whelan: "Electron Microscopy of Thin Crystals," (Butterworths, Washington, 1965) p. 12.

16. G. W. Groves and M. J. Whelan: Phil. Mag. $\underline{7}$, 1603 (1962).

17. P. B. Hirsch, A. Howie and M. J. Whelan: Phil. Trans. Roy. Soc., A252, 499 (1960).

18. M. E. Ashby and L. M. Brown: Phil. Mag. $\underline{8}$, 1083 (1963).

19. R. S. Barnes: Proc. Intern. Conf. on Crystal Lattice Defects, J. Phys. Soc. Japan $\underline{18}$, Supplement III, p. 305 (1963).
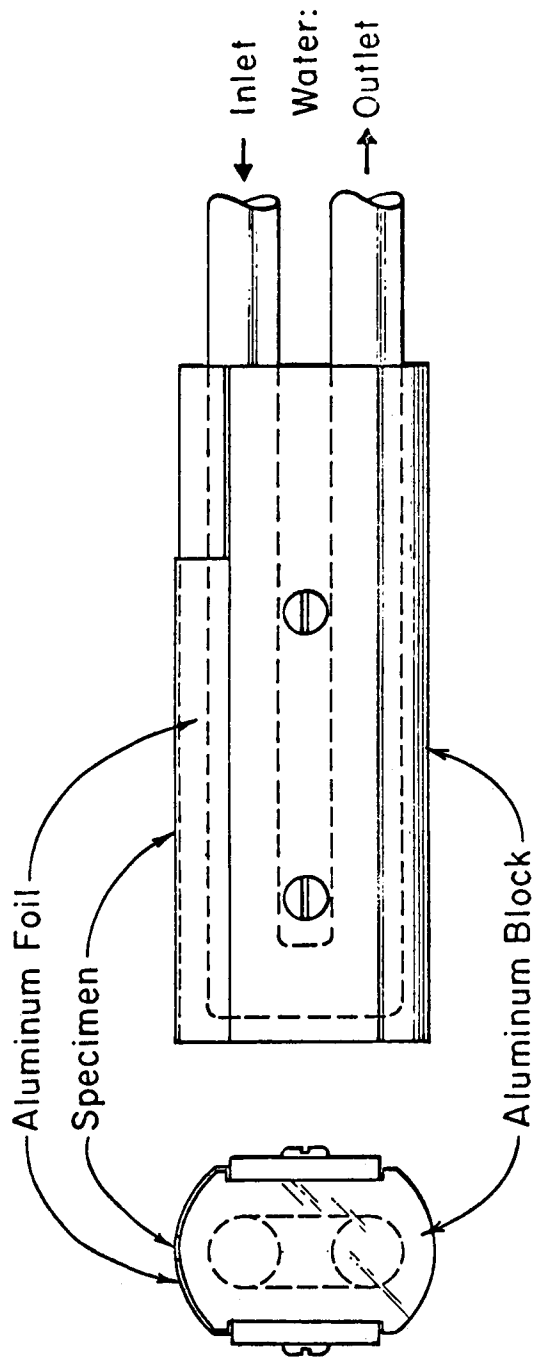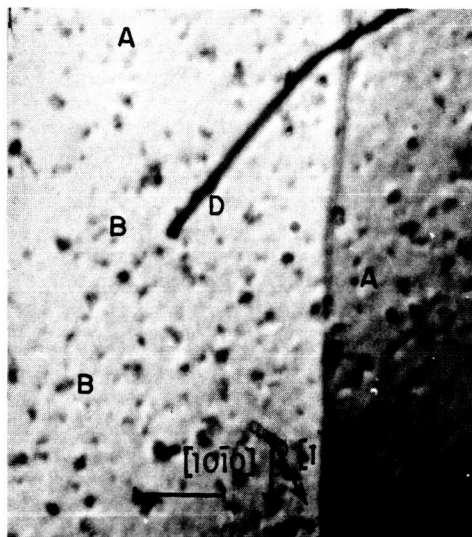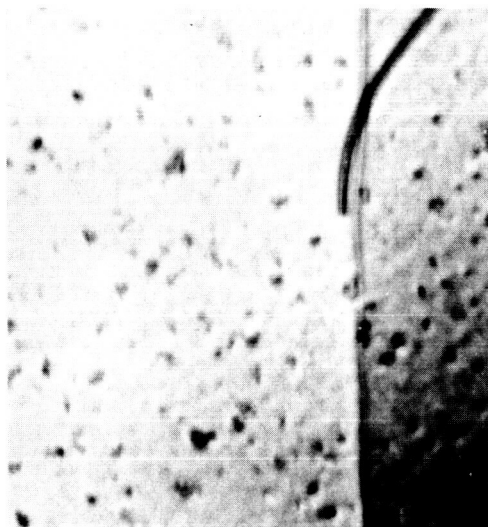
Fig. I   Water cooled target support for irradiating specimens.
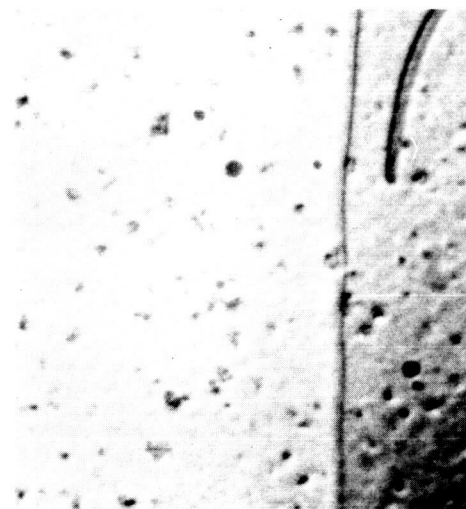
(a)

(b)

(c)

(d)

Fig. 2.   Defect clusters in proton-irradiated Bi_2Te_3.   Electron
micrographs taken after approximately 30 second intervals.   Areas
marked A and B show some of the defect clusters aligned along the
$\langle11\bar{2}0\rangle$ and $\langle10\bar{1}0\rangle$ directions, respectively.   The dislocation marked C
remains unchanged; the dislocation marked D reduces its length.
Length of the mark: 2,000 A.U.   Flux level: 1.8×10^{13} protons/
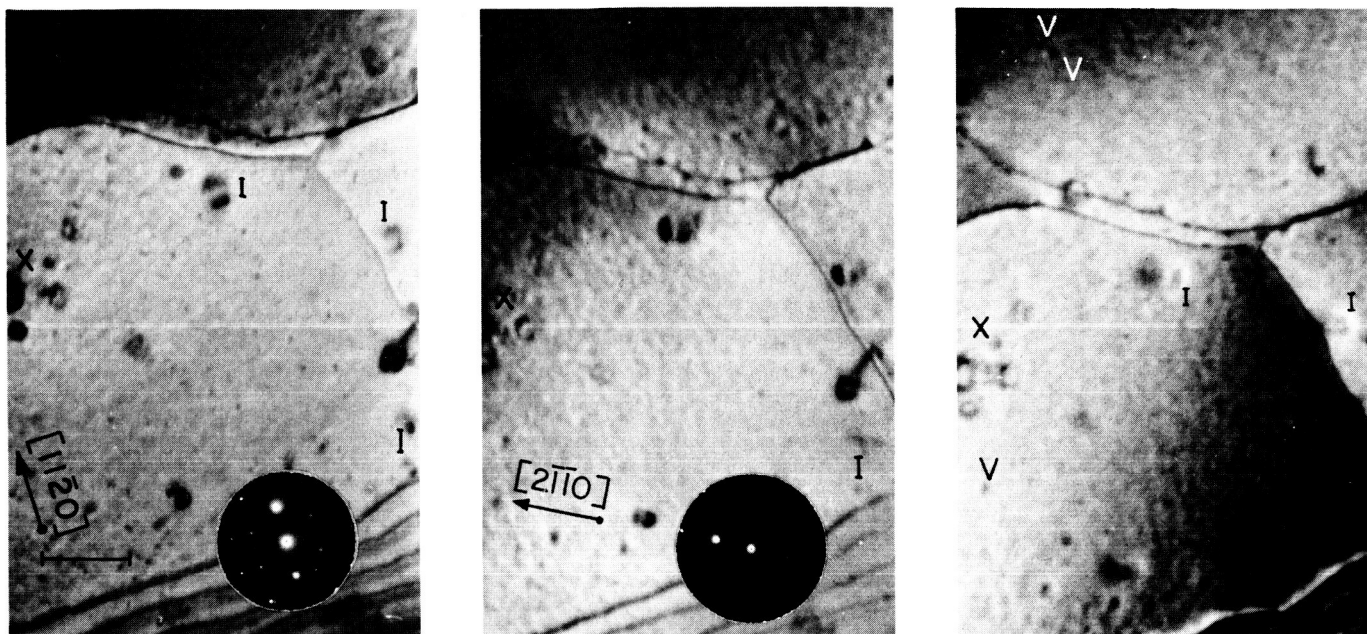cm^2-sec.   Integrated dose: 5.5×10^{18} protons/cm^2.
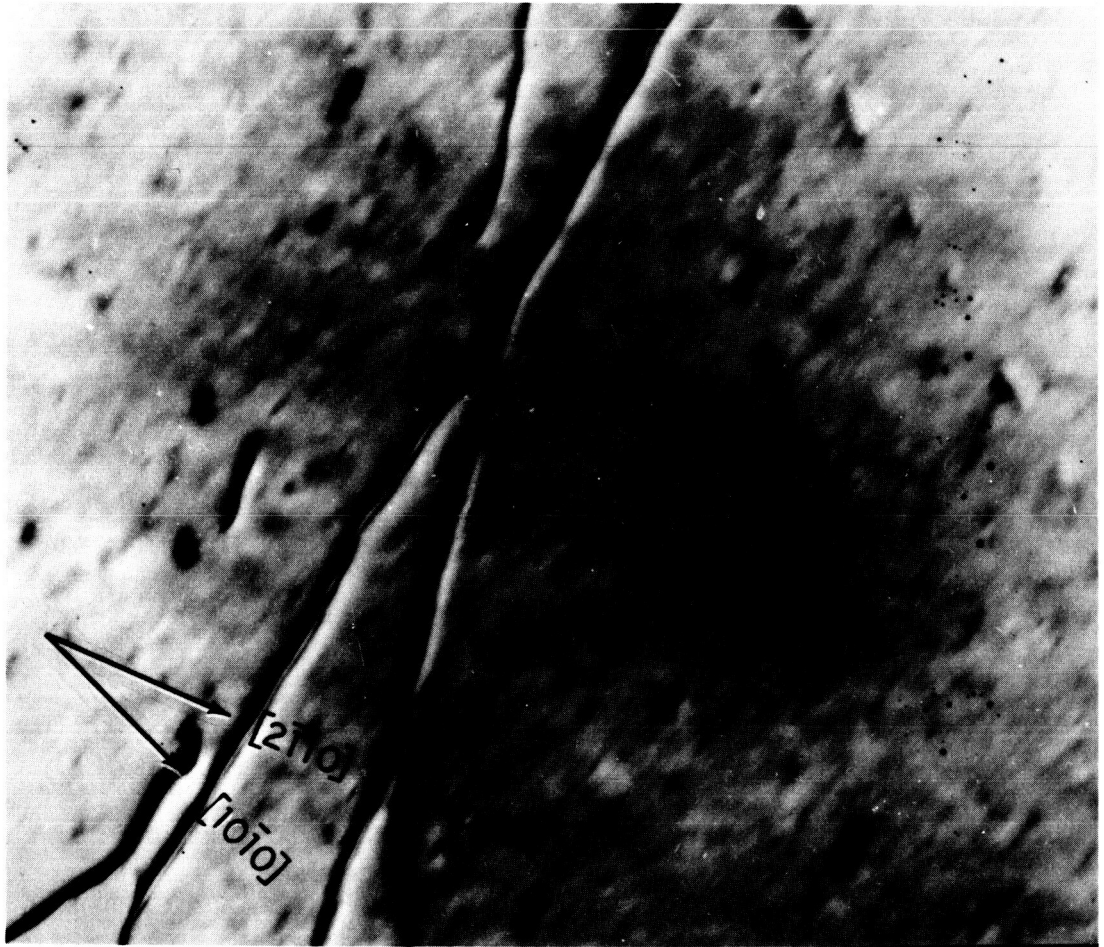
Fig. 3. Dislocation loops in proton-irradiated Bi_2Te_3. The major axis of the loops is aligned along the $\langle 11\bar{2}0 \rangle$ direction. Length of the mark: 2,000 A.U. Flux level: 1.8×10^{13} protons/cm^2-sec. Integrated dose: 5.5×10^{18} protons/cm^2.

(a)   (b)   (c)

Fig. 4. Defect clusters in proton-irradiated Bi_2Te_3. Electron micrographs taken for two diffraction vectors. Length of the mark: 2,000 A.U. Flux level: 3.0×10^{13} protons/cm^2-sec. Integrated dose: 5.5×10^{18} protons/cm^2.

(a) Bright-field image corresponding to a reflection from ($11\bar{2}0$) type planes. The line of no contrast of the defect clusters marked I is normal to the diffraction vector.

(b) Bright-field image corresponding to a reflection from ($2\bar{1}\bar{1}0$) type planes. The line of no contrast in the defects marked I has rotated so that it is normal to the diffraction vector.

(c) Dark-field image of (b). Note that the light side of the image from the clusters is in the opposite direction for the defect clusters marked I and V.
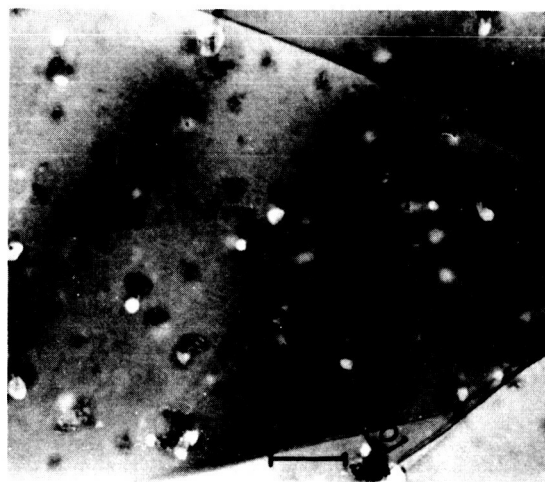
(a)
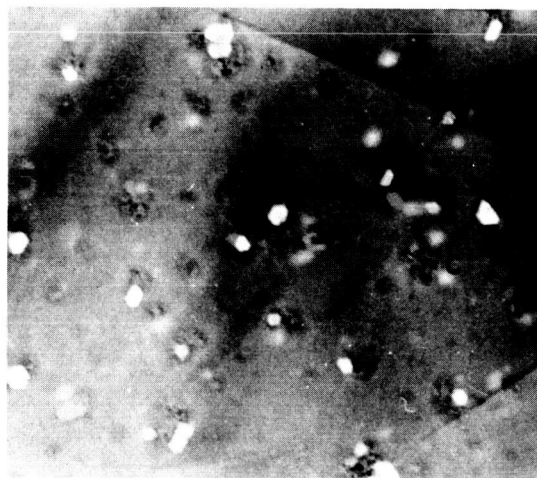
(b)
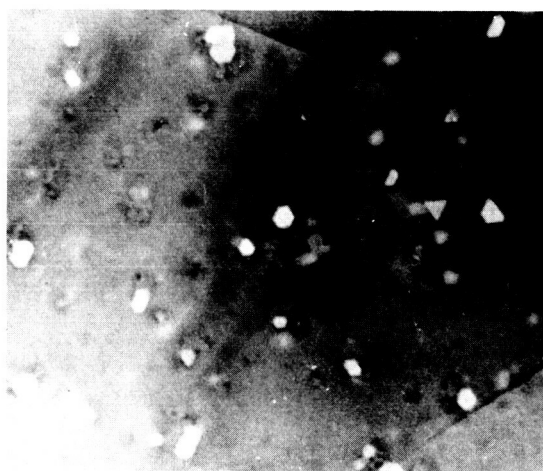
(c)

Fig. 5. Growth of hexagonal areas during observation in the electron microscope in proton-irradiated Bi_2Te_3. Regions marked A, B and C are growing with time. In region marked A, the hexagonal areas have assumed triangular shapes. The sides of the hexagonal and triangular areas are parallel to $\langle 11\bar{2}0 \rangle$ directions. Length of the mark: 2,000 A.U. Flux level: 3.0×10^{13} protons/ cm^2-sec. Integrated dose: 5.5×10^{18} protons/cm^2.
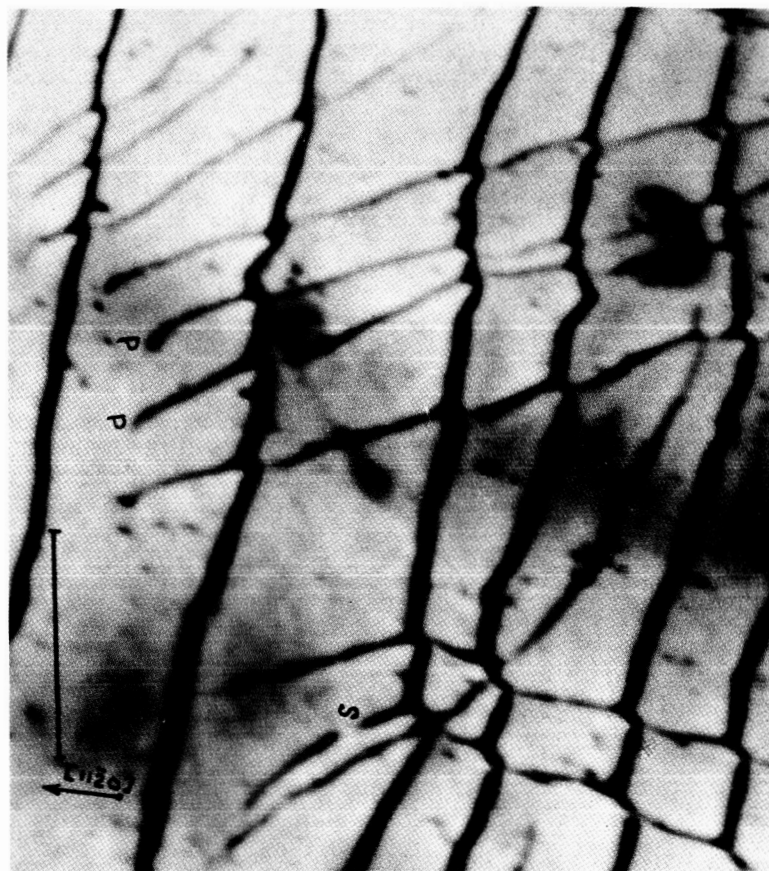
Fig. 6. Effect of proton irradiation on dislocation and dis-
location networks. At the segment marked S, the dislocation
line is out of contrast. Length of the mark: 2,000 A.U.
Flux level: 1.8 x 10^{13} protons/cm^2-sec. Integrated dose:
5.5 x 10^{18} protons/cm^2.